ORIGINAL PAPER

Comparative measurements of mineral elements in milk powders with laser-induced breakdown spectroscopy and inductively coupled plasma atomic emission spectroscopy

W. Q. Lei · J. El Haddad · V. Motto-Ros ·
N. Gilon-Delepine · A. Stankova · Q. L. Ma · X. S. Bai ·
L. J. Zheng · H. P. Zeng · J. Yu

Abstract Mineral elements contained in commercially available milk powders, including seven infant formulae and one adult milk, were analyzed with inductively coupled plasma atomic emission spectrometry (ICP-AES) and laser-induced breakdown spectroscopy (LIBS). The purpose of this work was, through a direct comparison of the analytical results, to provide an assessment of the performance of LIBS, and especially of the procedure of calibration-free LIBS (CF-LIBS), to deal with organic compounds such as milk powders. In our experiments, the matrix effect was clearly observed affecting the analytical results each time laser ablation was employed for sampling. Such effect was in addition directly observed by determining the physical parameters of the plasmas induced on the different samples. The CF-LIBS procedure was implemented to deduce the concentrations of Mg and K with Ca as the internal reference element. Quantitative analytical results with CF-LIBS were validated with ICP-AES measurements and nominal concentrations specified for commercial milks. The obtained good results with the CF-LIBS procedure demonstrate its capacity to take into account the difference in physical parameters of the plasma in the calculation of the concentrations of mineral elements, which allows a significant reduction of the matrix effect related to laser ablation. We finally discuss the way to optimize the implementation of the CF-LIBS procedure for the analysis of mineral elements in organic materials.

Keywords LIBS · CF-LIBS · ICP-AES · Matrix effect · Milk powder

W. Q. Lei · J. El Haddad · V. Motto-Ros · Q. L. Ma · J. Yu (✉)
Université de Lyon, Université Lyon 1, Villeurbanne, CNRS,
UMR5579, LASIM,
69622 Lyon, France
e-mail: jin.yu@lasim.univ-lyon1.fr

J. El Haddad · N. Gilon-Delepine · A. Stankova
Université de Lyon, Université Lyon 1, Villeurbanne, CNRS,
UMR5180, LSA,
69622 Lyon, France

W. Q. Lei · X. S. Bai · L. J. Zheng · H. P. Zeng
State Key Laboratory of Precision Spectroscopy,
East China Normal University,
Shanghai 200062, China

Introduction

Among available elemental analysis techniques, laser-induced breakdown spectroscopy (LIBS) exhibits attractive features, such as sensitive multi-elemental detection, rapid response for online monitoring, easy sample preparation for in situ measurements, high spatial resolution for surface mapping, and standoff operation capacity for remote sensing [1, 2]. These features have been triggering more and more attention for its applications in various domains [3, 4]. Quantitative analytical performance has been extensively demonstrated for metallic alloys thanks to a good understanding of the plasma generated from metallic matrix [3–6]. Reliable calibration curves can be established with reference samples which are easily available commercially [7, 8]. On the other hand, a calibration-free procedure (CF-LIBS) has been developed to extract elemental concentrations from LIBS spectra by assuming that the local thermodynamic equilibrium (LTE) is verified in the plasma [9–11]. Applications of LIBS to organic materials

were reported more recently, including qualitative analysis [12–14] and quantitative measurements [15–17]. Compared with metallic alloys, stronger matrix effects are unfortunately expected, which makes the preparation of matrix-matched reference samples very difficult [18, 19]. One of the solutions to be explored is the use of the CF-LIBS procedure which allows in principal the extraction of the concentrations of the analytes independently on the matrix in which they are embedded. The successful use of this procedure for metallic alloys [20] and its application to a number of other materials such as glasses [21], biomaterials [22], oxides [23], minerals [24], and soils [25], allow us to expect its good performance for organic samples in general and especially for taking into account the corrections made necessary by the matrix effect, in the calculation of the concentrations of mineral elements in an organic matrix. The question however concerns the LTE in a plasma induced from an organic matrix. In our previous work, on the characterization of the plasma induced from an organic sample, such as a potato, we have demonstrated that the LTE can be established over a certain period after the laser impact on the sample [26]. It is therefore possible to apply the CF-LIBS procedure to organic samples by detecting the plasma emission in this time interval. The aim of this work is thus to develop the calibration-free quantification procedure with LIBS for the analysis of mineral elements in milk powders including infant formulae. The obtained quantitative analysis results are compared with those obtained with the classical procedure, digestion step followed by inductively coupled plasma atomic emission spectroscopy (ICP-AES) analysis. Such direct comparison provides an assessment of the performance of LIBS, and especially of the procedure of CF-LIBS, to deal with organic compounds such as milk powders.

The organic compound analyzed in this work, milk powder, is an essential foodstuff for which it is important to develop sensitive and rapid elemental analysis techniques to quantitatively determine the concentrations of mineral elements contained in it. Such analysis is needed for food security as well as nutrition reasons especially for infant formulae which contain essential nutrients necessary for child growth. To develop an analytical procedure, milk powders can be easily digested using the classical procedure with nitric acid and microwave heating to obtain solutions with further quantification using ICP-AES. Milk powders are also easy to be prepared in pellets for LIBS measurements, with or without binder. In addition, milk powders for infant and adult are commercially available and provided together with indications of concentrations of many mineral elements. It must be however noticed that the commercial milks are not reference samples. Nevertheless, the indicative concentrations are often quite reliable. The determination of the concentrations of mineral elements in

milk powders with ICP-AES is a well-established procedure since 1980s [27–29]. Very recently, LIBS technique was applied to breakfast cereals for the determination of calcium concentration using the calibration curve method with a validation by ICP-AES [30]. Some recent works report the direct comparison between ICP-AES and LIBS for analysis of organic samples such as plants [31, 32]. Comparing the analytical performances of these different techniques for the quantitative analysis of mineral elements in milk powders is also the motivation of the present work.

In the following, after a brief presentation of the analyzed samples, the used setups and measurement protocols, the calibration curves established with the reference samples for ICP-AES and LIBS will be presented. The calibration curves were then applied for quantitative analysis of mineral elements in commercial milk powders using LIBS. Observed large discrepancies between the measured concentrations and the nominal values given by the providers of the milks suggested a strong matrix effect in laser ablation. The matrix effect was further confirmed by the determinations of the electron density and the temperature of the plasma and the observation of laser-induced craters. The analytical results with the CF-LIBS procedure will be then presented. The good agreements of the obtained results with respect to either the nominal concentrations or the measurements with ICP-AES demonstrated the reduction of the matrix effect by the CF-LIBS procedure. We will finally point out the possible improvements of the experimental setup to optimize the implementation of the CF-LIBS procedure for organic materials.

Sample preparations, experimental setups, and measurement protocols

Analyzed samples and preparation of pellets

Different milk powders were analyzed in this work, including eight commercially available products and a certified reference sample (BCR063 from IRMM). Among the eight commercial products, there were seven formulae for baby (Gallia, Guiggoz, Lemiel, Milupa, Novalac Bleu, Novalac Rose, Nutricia) and a skimmed milk powder for adult (Auchan), all from a local supermarket. In addition, we prepared several combined samples by mixing the reference sample and a powder of cellulose (04227BE-296 from Sigma Aldrich) with grain size ~20 μm at different percentages. The mixing percentages and the corresponding concentrations for Na, Mg, K, and Ca in the resulted mixtures are given in Table 1. The mixed powders as well as the commercial milk powders were pressed to obtain pellets with a 13-mm diameter using a hydraulic press (3 min under 10 tons). The pellets resulted from the

Table 1 Mixing percentages and the corresponding concentrations for Na, Mg, K, and Ca in the resulted mixtures

Percentage of the reference milk (%)	Concentration (mg/g)			
	K	Ca	Na	Mg
0	0.0	0.0	0.0	0.0
20	3.6	2.7	0.9	0.3
40	7.2	5.5	1.8	0.5
50	8.8	6.7	2.2	0.6
60	10.6	8.1	2.6	0.8
80	14.2	10.8	3.5	1.0
100	17.7	13.5	4.4	1.3

mixtures between the reference sample and cellulose were used as calibration standards for establishing the calibration curves for LIBS experiments. The same protocol has been successfully employed in our previous works to obtain standards for measurements with LIBS and laser ablation inductively coupled plasma mass spectrometry (LA-ICP-MS) [33, 34]. The preparation of the powders into pellets was necessary to have better ablation efficiency and higher repeatability of LIBS measurements.

Optimized wet digestion procedure

For the digestion of milk powders, a microwave-assisted nitric acid digestion procedure was developed using a microwave system (Mars Xpress, CEM μWave S.A.S). For the analysis of major elements, Na, Mg, K, and Ca, 100 mg of powder was placed in a closed vessel with analytical grade nitric acid. Five replicates were prepared for each sample in order to check the repeatability of the mineralisation procedure. In order to evaluate possible contaminations of the vessel, a nitric acid blank was analysed in several replicates. The optimisation of the digestion was made using the reference sample BCR063. The optimized temperature program was as the following: during the first 15 min the temperature rose from the room temperature to 200 °C which was kept for another 15 min. The optimal recovery was obtained for a power of 400 W. After cooling, the digests were diluted up to 50 ml with deionized water. The same dilution protocol was successfully employed in our previous works to obtain standards for measurements with LIBS and LA-ICP-MS [33, 34].

ICP-AES operation conditions

Measurements were made using an ICP-AES, JY 138 Ultrace (Jobin Yvon Horiba) modified for axial viewing. The spectral resolution was 4 p.m. in UV and 8 p.m. in the

visible. Two photomultipliers were available for the spectral coverage of 190–800 nm. The used operational parameters include a generator frequency of 40.68 MHz, an incident power of 1,075 W, a plasma gas flow of 12 l/min, an auxiliary flow of 0.15 l/min, a nebulizer gas flow of 0.65 l/min, and a solution uptake of 1 ml/min. The ICP-AES was calibrated using classical standard solutions prepared from stock solutions (Sigma-Aldrich).

ICP-AES analysis

The commercial milk powders contain a wide range of mineral elements including, Na, Mg, K, Ca, and P with concentrations larger than tens of milligrams per kilogram. The optimized digestion procedure allowed quantitative recoveries with acceptable uncertainties for Ca (108%, $RSD_{n=5}$=7%), K (98%, $RSD_{n=5}$=2%), Mg (106%, $RSD_{n=5}$=1.02%), and P (99%, $RSD_{n=5}$=4%) with the reference sample. An overestimation was observed for Na (115%, $RSD_{n=5}$=13%). A vessel or laboratory contamination could be suspected as Na is a very easily contaminating element. The following study was therefore focused on the three elements Mg, K, and Ca. According to the developed digestion protocol, their concentrations in the infant formulae and the adult milk powder were determined as presented in Table 2. The retrieved concentrations are in good agreement with the indicative values (nominal values).

Setup and protocol for LIBS measurements

A standard LIBS experimental setup was used in the present investigation. Its detailed description can be found elsewhere [26]. Briefly, the ablation source was a Q-switched Nd:YAG laser (Quantel Brillant) operating at 355 nm with a repetition rate of 10 Hz, pulse duration of 5 ns, and pulse energy of 50 mJ. The use of UV laser pulses increases the ablation efficiency of organic compounds such as milk powders. The laser beam was focused on the sample surface using a quartz lens of 5-cm focal length to generate the plasma. The sample pellet was moved using a stepper motor during the spectral accumulation in such way that each laser shot had a fresh sample surface. The beam size on the sample surface was estimated to be 500 μm by measuring the crater on the sample surface. The fluence on the sample surface was thus 25.5 J/cm^2 corresponding to a maximum irradiance of 5.1 GW/cm^2 without considering the absorption by the plasma. The emission from the plasma was collimated by a pair of parabolic mirrors which focused the emission into the entrance of an optical fiber of 50 μm core diameter. The use of mirrors to collect the plasma emission reduces the chromatic ablation and offers a large numerical aperture of the detection. The fiber coupled the plasma emission into an echelle spectrometer

Table 2 Elemental concentrations in milligrams per gram in the analyzed milk powders obtained after wet digestion and ICP-AES determination

Concentration (mg/g)	Mg			K			Ca		
	Nominal	ICP-AES	Relative deviation (%)	Nominal	ICP-AES	Relative deviation (%)	Nominal	ICP-AES	Relative deviation (%)
BCR063R	1.26	1.34	6.3	17.68	17.38	1.7	13.49	14.51	7.6
Gallia	0.42	0.41	2.4	4.92	4.96	0.8	3.86	4.35	12.7
Guigoz	0.54	0.57	5.6	6.45	6.53	1.2	5.35	5.93	10.8
Lemiel	0.55	0.63	14.5	5.8	5.73	1.2	5.6	5.92	5.7
Milupa	0.33	0.34	3.0	4.15	3.62	12.8	4.22	4.67	10.7
Novalac Bleu	0.45	0.53	17.8	4.7	4.8	2.1	3.8	4.24	11.6
Novalac Rose	0.45	0.48	6.7	6.25	6.75	8.0	5	5.61	12.2
Nutricia	0.6	0.6	0.0	6.3	6.74	7.0	5.5	6.25	13.6
Auchan	1.14	1.19	4.4	–	17.48	–	12.6	13.35	6.0

(Mechelle, Andor Technology) equipped with an intensified charge-coupled device (ICCD; iStar, Andor Technology). The detection system offered a spectral range between 240 and 820 nm and a resolution power of $\lambda/\Delta\lambda = 5,000$. Each spectrum was recorded by accumulating 60 laser shots. And for each sample, ten spectra were measured to evaluate the standard deviation. During the experiment, the lens-to-sample distance was controlled using a locking system with the use of a laser pointer and a CCD camera. In order to have a plasma in the local thermodynamic equilibrium (LTE) and at the same time a high signal-to-noise ratio for the spectrum detection, the position of the detection window was studied and found optimal from 1,000 to 4,000 ns after the impact of the laser pulse. This point will be discussed in details later in this paper.

Experimental results and discussions

Calibration curves for ICP-AES and LIBS

As an example, we show in Fig.1, the calibration curves with Ca II 317.9-nm line established for ICP-AES and LIBS. The ICP-AES calibration curve (Fig. 1a) established with classical aqueous standards showed an excellent linearity with a coefficient of determination of 0.9996. Similar results were obtained for other elements, 0.9995 for Mg and 0.996 for K. The calibration curve for LIBS, established using the prepared standards with mixture between the reference sample and cellulose, exhibits a linearity but with a smaller coefficient of determination of 0.98 as shown in Fig.1b. For Mg I 517.2-nm and K I 404.7-nm lines, we got coefficients of determination of 0.971 and 0.989, respectively, for the LIBS measurement. Self-absorption was checked for the above used lines with the procedure described in Ref. [35], we did not observed any noticed effect. The degradation of
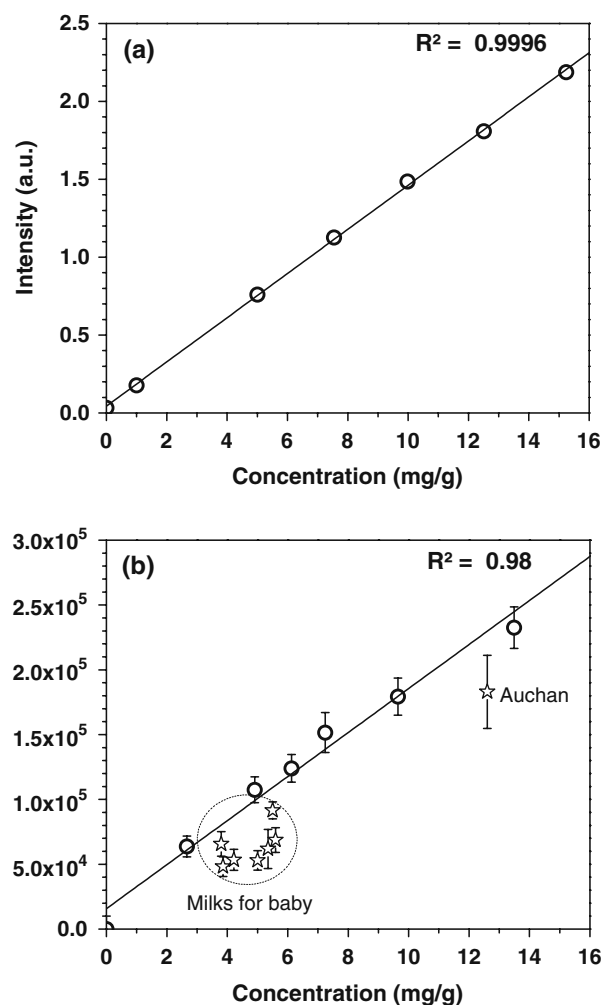

Fig. 1 Calibration curves with Ca II 317.9-nm line for **a** ICP-AES and **b** LIBS. The experimental points are represented by *circles*. The *stars* in (**b**) correspond to commercial milks and will be commented later

the coefficient of determination can be related to the fluctuation of the properties of the plasma in terms of the electron density, the temperature and the stoichiometry. This behavior indicates that the matrix-dependent interaction between laser and sample (the matrix effect) affected the physical-chemical properties of the plasma and subsequently the analytical signal. In Fig. 1b, the points measured from commercial milk samples are also plotted. We will come back later for detailed comments of these points.

Quantitative measurements with LIBS using calibration curves

Calibration curves (Fig. 1b for Ca) were used to determine the concentrations of Ca, K, and Mg in the commercial milks. In the LIBS spectra of the samples, Ca II 317.9-nm, K I 404.7-nm, and Mg I 517.2-nm lines were used, respectively. Figure 2 shows the results, where the concentrations from LIBS calibration curve measurement are presented in comparison with the nominal values and the concentrations measured with ICP-AES. The error bars in the figures represent the standard deviations of the measurements. Each concentration measured with LIBS is the average of ten measures performed within 1 h of time interval. The standard deviations indicate therefore the repeatability of the measurement. From the presented results, we can see first, the standard deviations of the LIBS measurements are in general much larger than those of ICP-AES measurements. The averaged error bars across all the samples were respectively 3.2%, 3.6%, and 4.0%, for Mg, K, and Ca for ICP-AES measurements, while these values become 17%, 9.6%, and 5.8% for LIBS measurements. The repeatability of the measurement is thus degraded for LIBS analysis. This lower repeatability can be considered as due to the higher sensitivity of the LIBS signal to the experimental fluctuations, such as laser energy instability. We can also remark that the averaged concentrations determined by LIBS are systematically lower than the nominal values, with an averaged bias across all samples of 52.8% for Mg, 42.3% for K and 38.0% for Ca. These deviations are significantly larger than those observed for ICP-AES measurements, 6.2% for Mg, 4.9% for K, and 10% for Ca, which is consistent with dispersions of the actual concentrations in commercial milks with respect to the nominal values. The observed systematical deviation of the LIBS measurements to significant lower values suggests a strong matrix effect which leads to a significant difference in plasma property for the commercial milks compared with the prepared calibration standards. This matrix effect can also be observed in Fig. 1b where the plasma emission intensities (Ca II 317.9 nm) for the eight commercial milks are plotted against their nominal calcium concentration (the stars in Fig. 1b). It is clear that all the
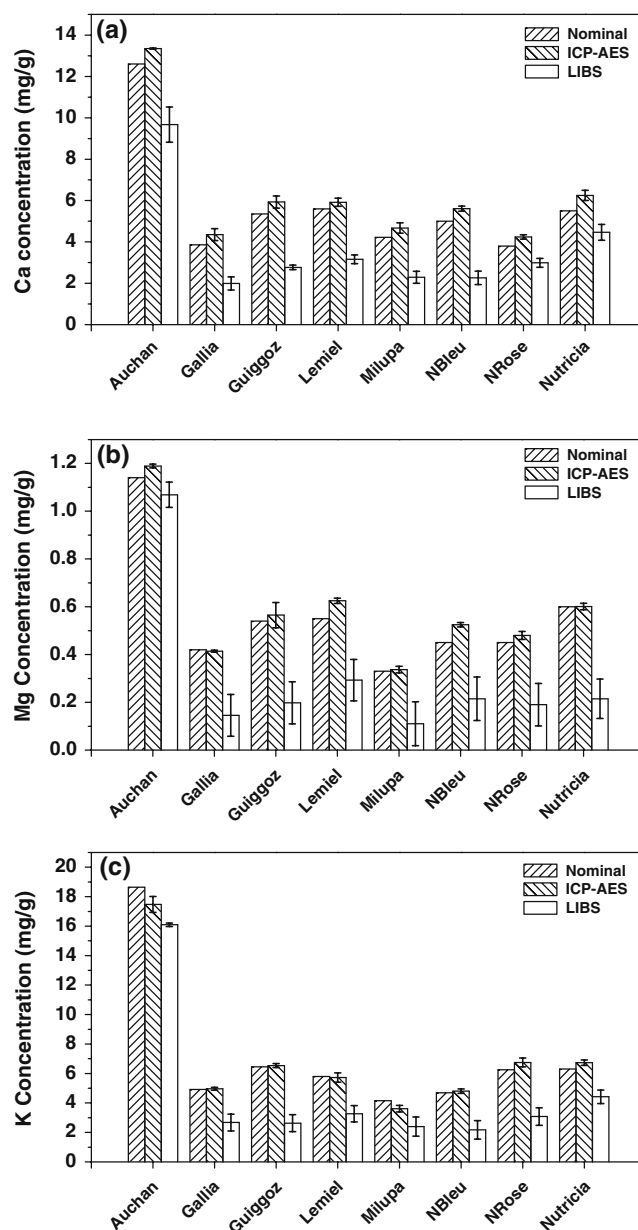

Fig. 2 Quantitative analysis results with LIBS using calibration curves compared with the measurements with ICP-AES and the nominal concentrations for different commercial milks

obtained points lie under the calibration curve with significant deviations.

Direct observations of the matrix effect in laser ablation

In order to confirm our hypothesis of matrix effect to explain the systematic deviations of the concentrations measured with LIBS for commercial milks with respect to the nominal values, we have measured the physical parameters of the plasma, the electron density and the temperature, for all analyzed samples. The electron density was determined using the Stark broadening of the Hα line

at 656.3 nm, and the temperature was extracted from the Saha–Boltzmann plot (SBP) using a set of calcium lines. The line selection is very important for plasma diagnostics. The use of the Hα line for electron density determination has been extensively reported because it is well isolated and broadened by a strong linear Stark effect [36, 37]. The self-absorption is apparently absent in our measurements for this line. For temperature determination, the used lines have not to be affected by self-absorption. Growth curves were used to check the linearity of the intensities of the chosen calcium lines in the spectra obtained with the prepared reference samples as functions of the calcium concentration. Figure 3 shows the growth curves of several calcium lines used for the temperature determination. Here, the intensity corresponds to the surface under an emission line. We can see that all the chosen calcium lines have a linear response to the concentration within the range from 0 to 14 mg/g. Such range overlaps the calcium concentrations of all the analyzed samples. We can therefore use these lines for temperature determination without the influence of self-absorption. Finally, for the pure cellulose sample, the vibrational temperature was extracted from the emission band heads of CN molecule.

Electron density and temperature were thus determined for the 15 analyzed samples, among them the certified sample, the pure cellulose sample, the five prepared standards (cellulose/BCR063 mixtures), and the eight commercial milks. As shown in Fig. 4, the electron density and the temperature vary among the different samples ablated in the same condition. The matrix effect is therefore obvious for LIBS measurements. The reference sample BCR063 and the cellulose/BCR063 mixtures exhibit quite close values of temperature with a slight increase (from ~8,300 to ~8,750 K)
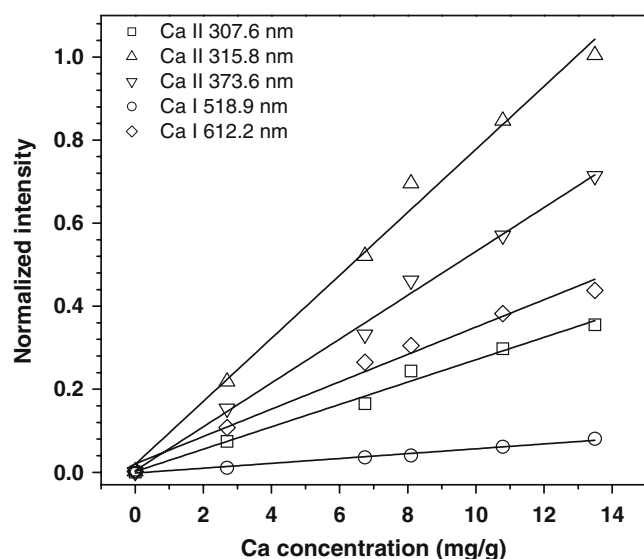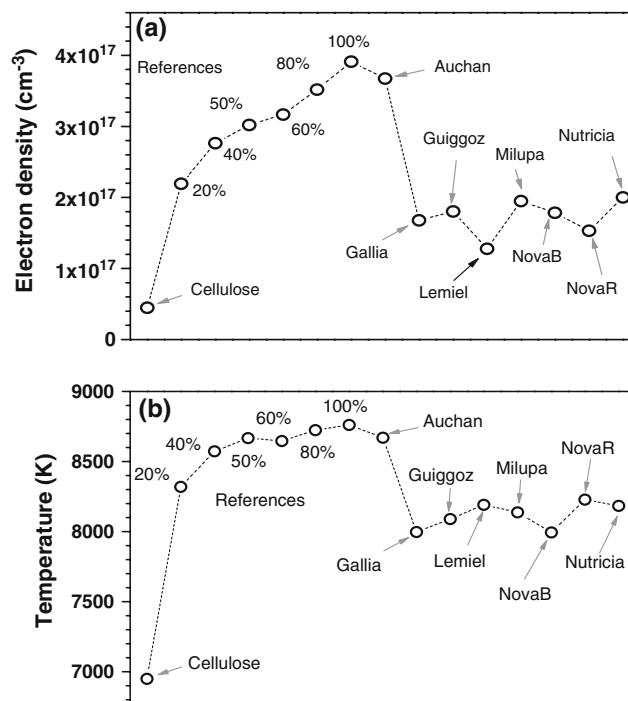

Fig. 4 Electron densities and temperatures of the laser-induced plasma measured for different analyzed samples

as a function of the concentration, with an average and a standard deviation of 8,600±160 K. The electron density for these samples shows a regular increase (from ~2.2×10^{17} to ~3.9×10^{17} cm^{-3}) as a function of the concentration with an average and a standard deviation of $(3.1 \pm 0.5) \times 10^{17}$ cm^{-3}. For the commercial milks, except the "Auchan" sample, a similar temperature is observed, 8,000±230K. This temperature is significantly lower than those of the reference samples. Concerning the electron density, a similar value of $(1.8 \pm 0.3) \times 10^{17}$ cm^{-3} is observed for all commercial milks except the "Auchan" one. Again, the electron density observed is significantly lower than those of the reference samples. The "Auchan" sample is thus an exception among the commercial milks. The temperature and electron density measured for it, 8670 K and 3.7×10^{17} cm^{-3} are in the ranges of the values measured for the reference samples. We can remark that the electron density and also the temperature of the plasma are directly correlated to the concentrations of mineral elements, Ca and K for example, in milk samples.

These observations can be now used to explain the results shown in Figs. 1b and 2, where we remarked that for the commercial milks, the measured spectral intensities for the given nominal concentrations or the measured concentrations deduced from the calibration curves are systematically and significantly lower than the expected values. In fact, the electron density and the temperature of the plasma induced from these samples are lower than those for the prepared reference samples which were used to establish the calibration curves. These deviations are however

Fig. 3 Growth curves of the calcium lines used for the determination of the plasma temperature

reduced for the "Auchan" sample (Fig. 4a, b). This exception can be now understood because the electron density and the temperature of this sample are different from those of the other commercial milks and lie in the ranges of the reference samples.

The matrix effect was further directly observed from the images of the craters on the different samples as shown in Fig. 5. We observe similar craters at the surfaces after ablation for the pure cellulose, the pure certified reference and the "Auchan" sample. However, the surface of the "Guigoz" sample, one of the commercial milks for baby exhibits a totally different aspect. The total destruction of its surface with the disappearance of distinguished individual craters indicates a surface mechanical resistance against laser ablation much weaker than that of the reference samples. Such weaker mechanical resistance can lead to a resulted plasma with lower electron density and temperature as observed in our experiments.

Consequently, the matrix effect must be taken into account in order to achieve accurate and precise analysis. In practice, matrix-matched reference samples need to be prepared. Our experiments show however the difficulty to have such reference samples especially for organic materials. Even for a same type of matrix, milk powders for instance, the matrix effect is obvious, leading to the impossibility to apply the calibration curves. The origin of the matrix effect can be multiple physical and chemical reasons. For organic materials, it can be in particular related to the mineral elements present in small concentrations in the matrix, as we observed in our experiments. The absorption of an organic material can be significantly increased with the presence of mineral elements. These elements can be easily ionized by laser radiation leading to free electrons available for further absorption of laser
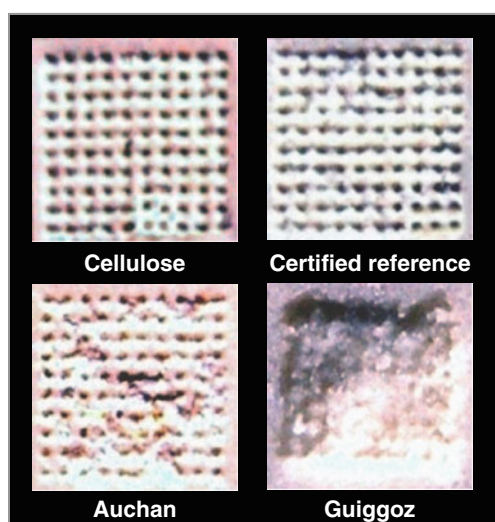

Fig. 5 Photos of craters after laser ablation on the pellets of different samples

radiation. The correction of the matrix effect can be quite complex. However, as we show here, it can be quantified with the electron density and the temperature of the plasma, its effect may therefore be taken into account in the calculation of the concentrations. This is precisely the idea of the CF-LIBS procedure where the plasma parameters, in particular the temperature, are used in the calculation of the concentrations.

Quantitative measurement using CF-LIBS with an internal reference element

To employ the CF-LIBS procedure, the laser-induced plasma is assumed to be an ideal plasma [9]. In other words, basic hypotheses, such as stoichiometric ablation, optical thinness of the plasma and stationary plasma in the LTE (a unique constant temperature for all species in the plasma) are supposed to be verified. Moreover, we use here an element with known concentration as internal reference, since all the elements in the sample cannot be detected simultaneously for the normalization needed in the standard CF-LIBS procedure. Under such assumptions, the concentration of a specific element α, C_α, is related to that of the reference element, C_{ref} by the following expression:

$$\frac{C_\alpha}{C_{ref}} = \frac{M_\alpha}{M_{ref}} \cdot \frac{U_\alpha(1 + S_\alpha)}{U_{ref}(1 + S_{ref})} \exp(D_\alpha - D_{ref}) \qquad (1)$$

where D, M, and U refer to the intercept in SBP, the atomic weight and the partition function respectively with their subscripts specifying the concerned element, S is the ratio between the number densities of ions and the corresponding neutral atoms, which can be deduced from the Saha equation.

In our experiments, due to its relative high concentration in all samples and a large number of detected lines, calcium was chosen as the internal reference. In addition, proper choice of lines for CF-LIBS procedure is very important. These lines must be well isolated without interference with other emissions. They need to be detected with a good signal-to-noise ratio and without significant self-absorption. And finally, their spectroscopic data must be available. For Ca, several lines were chosen, including two Ca I lines at 428.3 and 518.9 nm and three ionic lines, Ca II 315.8, 317.9- and 373.6-nm lines. For Mg and K, 517.8- and 404.7-nm lines were used, respectively. All these lines were checked to be not self-absorbed by the linearity of the growth curves measured with the prepared reference samples. These lines, together with the electron density and the temperature determined above (Fig. 4) for different commercial milks, have allowed us to calculate the concentrations of magnesium and potassium in these samples with calcium as the internal reference. In order to determine the uncertainties of the measurements, the concentrations of Mg and K are calculat-

ed for each of the five lines of calcium mentioned above, which allows us to extract an averaged concentration with corresponding standard deviations.

The retrieved concentrations are shown in Fig.6. We can see that the concentrations for Mg and K extracted using the CF-LIBS procedure with an internal reference element are now in agreement with the nominal concentrations reported by the produces within the measurement uncertainties. Such uncertainties correspond to the standard deviations of the measurements and represented in the figures by the error bars. With respect to the nominal values, the averaged bias of the CF-LIBS measurements across all the samples are 17.6% and 12.1% for Mg and K, respectively, while the corresponding deviations for the LIBS measurement with calibration curves are 52.8% for Mg and 42.3% for K as shown above (Fig. 2b, c). Such improvement highlights an efficient compensation of the matrix effect by the CF-LIBS procedure as expected. The bias of the measurements with CF-LIBS remain however significantly larger than those of the measurement with ICP-AES, 6.4% for Mg and 4.4% for K with respect to the nominal values. In addition, when comparing the repeatability of the measurements, the averaged error bars across all the samples are 4.1% for Mg and 4.4% for K for the

ICP-AES measurements, while these values are 24% for Mg and 16% for K for the CF-LIBS measurements.

Discussions on the further improvements of the CF-LIBS procedure for organic materials

The fair accuracy of the measurements with CF-LIBS (larger bias than ICP-AES measurements) can be due to the deviation from the ideal conditions for applying the CF-LIBS procedure mentioned above. In fact, due to the transient nature of the plasma, a stationary LTE state can only be approximately realized for the plasma. Since the LIBS signal is always integrated over a time interval to get better signal-to-noise ratio, it is crucial to choose this time window (delay and width) to meet the requirement of the stationary LTE condition.

In our experiments, a detection window from 1,000 to 4,000 ns after the impact of the laser pulse was chosen for all LIBS measurements as mentioned above. Such detection window was chosen after the verification procedure described in our previous works [26]. The certified reference sample was used to study the evolution of the plasma. Firstly, the McWhirter criterion, which requires a minimal electron density of $N_e=1.23\times10^{16}$ cm^{-3} (calculated for $\Delta E=4$ eV and $T=10,000$ K) to ensure the necessary condition of the LTE, was checked with the evolution of the Hα line. Our measurement showed an electron density larger than this value up to a delay of 6,000 ns. The sufficient condition of the LTE for a transient plasma was checked by calculating different temperatures associated to the different species in the plasma. Atomic and ionic lines of calcium and molecular lines from cyano radicals CN were used in this study. The evolutions of the different temperature are shown in Fig. 7. We can see that the temperature retrieved from the Boltzmann plot of ionic
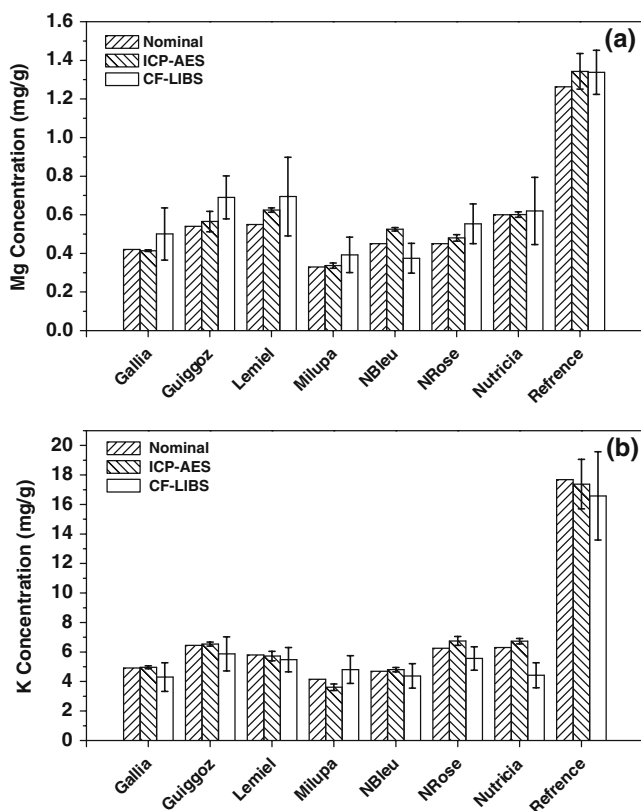

Fig. 6 Concentrations of Mg and K retrieved using the CF-LIBS procedure with Ca as the internal reference compared with the corresponding nominal values and the measurements with ICP-AES
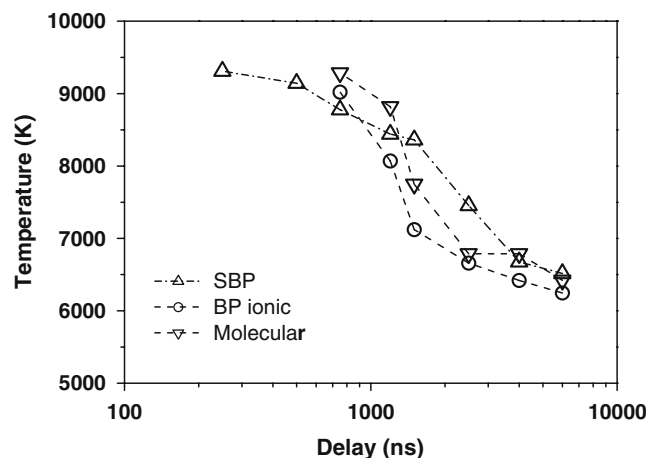

Fig. 7 Evolution of the temperatures of the different species in the plasma

lines and from the SBP merged together after about 1,000 ns. In addition, the molecular temperature retrieved from the vibration temperature of CN molecules (violet bands) exhibits the same tendency after the same delay. Before the delay of 750 ns, the ionic and molecular temperatures cannot be determined with enough precision in our experiments. However, our previous work [26] showed significant difference among these temperatures in shorter delays. We can thus consider the LTE state of the plasma for delays beyond 1,000 ns. We can however remark that in this interval, the temperature varied from ~8,500 to ~6,500 K. The integration of the LIBS signal over this interval only provides an approximation of a stationary plasma in LTE. This approximation may introduce inaccuracy in the determination of concentrations with CF-LIBS as we observed.

According to the above discussions, the search of a stationary LTE plasma is not compatible with the need of integrating the LIBS signal to increase the signal-to-noise ratio. A short integration time is in principal favorable for a more accurate measurement with the CF-LIBS procedure. However, a short integration time automatically degrades the signal-to-noise ratio of the LIBS signal. The attempt to have a stationary LTE plasma necessarily restricts the effective detection of the plasma emission in a limited time interval. Such restriction intrinsically reduces the sensitivity of the CF-LIBS procedure and makes its application more difficult for minor mineral elements with very low concentrations in an organic matrix.

In order to improve the performance of the CF-LIBS procedure for the quantitative analysis of mineral elements in organic materials, it is thus necessary to increase the sensitivity of the detection system. In our experiment, a compact echelle spectrometer was used. It offered a larger spectral range with high resolution. But it suffers from a relatively low detection sensitivity due to a small entrance port of 50-μm aperture limiting its throughput. The ideal detection system for an optimized implementation of the CF-LIBS procedure may consist of two parallel and simultaneous detection channels. A first channel (diagnostics channel) with a large spectral range but not necessarily with a high sensitivity, provides the simultaneous detections of the Hα line for electron density measurement and a large number of lines of a major element, calcium for example, for the precise determination of the temperature. A second channel (analysis channel) with higher detection sensitivity but narrower spectral range allows the line emissions from one or several minor elements to be detected with high signal-to-noise ratio. Our experiment shows that the diagnostics channel can be a combination of an echelle spectrometer and an ICCD, which provides satisfactory determination of the plasma parameters. For the analysis channel, a Czerny–Turner spectrometer for example, may be used for higher detection sensitivity with its high throughput. In practice however, the use of two separated spectrometers with two independent light collection systems may be restricting. Stack of compact monolithic spectrometers may provide a compromise of a wide spectral range and a high throughput [38]. Its use together with a time-resolved detection system may be interesting for quantitative analysis with the CF-LIBS procedure [39, 40].

Conclusions

In this work, we have measured the concentrations of mineral elements, in particular calcium, magnesium, and potassium, in milk powders with ICP-AES and LIBS. The comparison of the results from these two different analytical techniques has allowed assessment and validation of the CF-LIBS procedure applied to the quantitative analysis of mineral elements in an organic matrix, such as milk powders. Our results showed obvious matrix effect each time laser ablation was involved for sampling. We have observed in our experiments correlations between electron density/temperature of the plasma and the concentrations of mineral elements (Ca and K for example) in the sample. Such matrix effect made the established calibration curves difficult to be used for accurate quantitative analysis unless matrix-matched reference samples are available, a difficult task especially for organic materials.

Our results show furthermore that the plasma diagnostics provides a quantitative indication of the matrix effect in terms of the variations in electron density and temperature of the plasma. It is therefore expected that the CF-LIBS procedure contributes to the reduction of the matrix effect by taking into account the plasma parameters in the calculation of the concentrations. Such efficient compensation of the matrix effect has been demonstrated in our experiments for the determination of the concentrations of magnesium and potassium in commercial milk powders. The quantitative analytical results obtained from the CF-LIBS procedure remain however significantly less accurate than those obtained with ICP-AES. It is certainly possible to improve the experimental setup used in this work for an optimized implementation of CF-LIBS for organic materials by using, for example, two simultaneous detection channels respectively optimized for plasma diagnostics and for detection of weak emission from trace elements.

References

1. Cremers DA, Radziemski LJ (2006) Handbook of laser-induced breakdown spectroscopy. Wiely, Chichester

2. Miziolek AW, Palleschi V, Schechter I (eds) (2006) Laser-induced breakdown spectroscopy: fundamentals and applications. Cambridge University Press, Cambridge

3. Cremers DA, Chinni RC (2009) Laser-induced breakdown spectroscopy—capabilities and limitations. Appl Spectrosc Rev 44:457–506

4. Gaudiuso R, Dell'Aglio M, De Pascale O, Senesi GS, De Giacomo A (2010) Laser induced breakdown spectroscopy for elemental analysis in environmental, cultural heritage and space applications: a review of methods and results. Sensors 10:7434–7468

5. Corsi M, Cristoforetti G, Palleschi V, Salvetti A, Tognoni E (2001) A fast and accurate method for the determination of precious alloys caratage by laser induced plasma spectroscopy. Eur Phys J D 13:373–377

6. Bulajic D, Corsi M, Cristoforetti G, Legnaioli S, Palleschi V et al (2002) A procedure for correcting self-absorption in calibration free-laser induced breakdown spectroscopy. Spectrochim Acta B 57:339–353

7. Gornushkin IB, Anzano JM, King LA, Smith BW, Omenetto N et al (1999) Curve of growth methodology applied to laser-induced plasma emission spectroscopy. Spectrochim Acta B 54:491–503

8. Mohamed WTY (2008) Improved LIBS limit of detection of Be, Mg, Si, Mn, Fe and Cu in aluminum alloy samples using a portable Echelle spectrometer with ICCD camera. Opt Laser Technol 40:30–38

9. Ciucci A, Corsi M, Palleschi V, Rastelli S, Salvetti A et al (1999) New procedure for quantitative elemental analysis by laser-induced plasma spectroscopy. Appl Spectrosc 53:960–964

10. Fornarini L, Colao F, Fantoni R, Lazic V, Spizzicchino V (2005) Calibration analysis of bronze samples by nanosecond laser induced breakdown spectroscopy: a theoretical and experimental approach. Spectrochim Acta B 60:1186–1201

11. Herrera K, Tognoni E, Omenetto N, Gornushkin IB, Smith BW et al (2009) Comparative study of two standard-free approaches in laser-induced breakdown spectroscopy as applied to the quantitative analysis of aluminum alloy standards under vacuum conditions. J Anal At Spectrom 24:426–438

12. Portnov A, Rosenwaks S, Bar I (2003) Emission following laser-induced breakdown spectroscopy of organic compounds in ambient air. Appl Opt 42:2835–2842

13. Barbini R, Colao F, Fantoni R, Palucci A, Ribezzo S et al (1997) Semi-quantitative time resolved LIBS measurements. Appl Phys B 65:101–107

14. Juvé V, Portelli R, Boueri M, Baudelet M, Yu J (2008) Space-resolved analysis of trace elements in fresh vegetables using ultraviolet nanosecond laser-induced breakdown spectroscopy. Spectrochim Acta B 63:1047–1053

15. Pandhija S, Rai NK, Rai AK, Thakur SN (2010) Contaminant concentration in environment samples using LIBS and CF-LIBS. Appl Phys B 98:231–241

16. Corsi M, Cristoforetti G, Hidalgo M, Legnaioli S, Palleschi V (2003) Application of laser-induced breakdown spectroscopy technique to hair tissue mineral analysis. Appl Opt 42:6133–6137

17. Senesi GS, Dell'Aglio M, Gaudiuso R, De Giacomo A, Zaccone C et al (2009) Heavy metal concentrations in soils as determined by laser-induced breakdown spectroscopy (LIBS), with special emphasis on chromium. Environ Res 109:413–420

18. Eppler AS, Cremers DA, Hickmott DD, Ferris MJ, Koskelo AC (1996) Matrix effects in the detection of Pb and Ba in soils using laser-induced breakdown spectroscopy. Appl Spectrosc 50:1175–1181

19. Gornushkin SI, Gornushkin IB, Anzano JM, Smith BW, Winefordner JD (2002) Effective normalization technique for correction of matrix effects in laser-induced breakdown spectroscopy detection of magnesium in powdered samples. Appl Spectrosc 56:433–436

20. Tognoni E, Cristoforetti G, Legnaioli S, Palleschi V (2010) Calibration-free laser-induced breakdown spectroscopy: state of the art. Spectrochim Acta B 65:1–14

21. Burakov VS, Kiris VV, Naumenkov PA, Raikov SN (2004) Calibration-free laser spectral analysis of glasses and copper alloys. J Appl Spectrosc 71:740–746

22. Singh VK, Singh V, Rai AK, Thakur SN, Rai PK, Singh JP (2008) Quantitative analysis of gallstones using laser-induced breakdown spectroscopy. Appl Opt 47:G38–G47

23. Praher B, Palleschi V, Viskup V, Heitz J, Pedarnig JD JD (2010) Calibration free laser-induced breakdown spectroscopy of oxide materials, Spectrochim. Acta B 65:671–679

24. De Giacomo A, Dell'Aglio M, De Pascale O, Longo S, Capitelli M (2007) Laser induced breakdown spectroscopy on meteorites. Spectrochim Acta B 62:1606–1611

25. Herrera K, Tognoni E, Smith BW, Omenetto N, Winefordner JD (2009) Semiquantitative analysis of metal alloys, brass and soil samples by calibration-free laser-induced breakdown spectroscopy: recent results and considerations. J Anal At Spectrom 24:413–425

26. Lei WQ, Mottoros V, Boueri M, Ma QL, Zhang DC et al (2009) Time-resolved characterization of laser-induced plasma from fresh potatoes. Spectrochim Acta B 64:891–898

27. Schramel P (1983) Consideration of inductively coupled plasma spectroscopy for trace element analysis in the bio-medical and environmental fields. Spectrochim Acta B 38:199–206

28. Nobrega JA, Gelinas Y, Krushevska A (1997) Direct determination of major and trace elements in milk by inductively coupled plasma atomic emission and mass spectrometry. J Anal At Spectrom 12:1243–1246

29. McKinstry PJ, Indyk HE, Kim ND (1999) The determination of major and minor elements in milk and infant formula by slurry nebulisation and inductively coupled plasma-optical emission spectrometry (ICP-OES). Food Chem 65:245–252

30. Ferreira EC, Menezes EA, Matos WO, Milori DMBP, Nogueria ARA et al (2010) Determination of Ca in breakfast cereals by laser induced breakdown spectroscopy. Food Control 21:1327–1330

31. Trevizan LC Jr, DS SRE, Jr NDV, Nunes LC et al (2009) Evaluation of LIBS for the determination of micronutrients in plant materials. Spectrochim Acta B 64:369–377

32. Pouzar M, Cernohorsky T, Prusova M, Prokopcakova P, Krejcova A (2009) LIBS analysis of crop plants. J Anal At Spectrom 24:953–957

33. Stankova A, Dutruch L, Gilon N, Kanicky V (2011) Comparison of LA-ICP-MS and LA-ICP-OES for the analysis of some elements in fly ashes. J Anal At Spectrom (in press)

34. Stankova A, Dutruch L, Gilon N, Kanicky V (2010) A simple LIBS method for fast quantitative analysis of fly ashes. Fuel 89:3468–3474

35. El Sherbini AM, El Sherbini ThM, Hegazy H, Cristoforetti H, Legnaioli S, Palleschi V, Pardini L, Salvetti A, Tognoni E (2005) Evaluation of self-absorption coefficients of aluminum emission

lines in laser-induced breakdown spectroscopy measurements. Spectrochim Acta B 60:1573–1579

36. El Sherbini AM, Hegazy H, El Sherbini ThM (2006) Measurement of the electron density utilizing the Hα-line from laser produced plasma in air. Spectrochim Acta B 61:532–539

37. Griem HR (1974) Spectral line broadening by plasmas. Academic Press, New York

38. De Lucia FC Jr, Harmon RS, McNesby KL, Winkel RJ Jr, Miziolek AW (2003) Laser-induced breakdown spectroscopy analysis of energetic materials. Appl Optics 42:6148–6152

39. Sun L, Yu H (2009) Correction of self-absorption effect in calibration-free laser-induced breakdown spectroscopy by an internal reference method. Talanta 79:388–395

40. Pandhija S, Rai AK (2009) In situ multielemental monitoring in coral skeleton by CF-LIBS. Appl Phys B 94:545–552